Calderón Multiplicative Preconditioned EFIE With Perturbation Method

Sheng Sun, *Senior Member, IEEE*, Yang G. Liu, Weng Cho Chew, *Fellow, IEEE*, and Zuhui Ma

***Abstract*—In this paper, we address the low-frequency breakdown and inaccuracy problems in the Calderón multiplicative preconditioned electric field integral equation (CMP-EFIE) operator, and propose the perturbation method as a remedy for three-dimensional perfect electric conductor (PEC) scatterers. The electric currents at different frequency orders as a power series can be obtained accurately in a recursive manner by solving the same matrix system with updated right hand side vectors. This method does not either require a search for the loops in the loop-tree/-star based method or include charge as additional unknown in the augmented EFIE method. Numerical examples show the far-field pattern can be accurately computed at extremely low frequencies by the proposed perturbation method.**

***Index Terms*—Calderón multiplicative preconditioner (CMP), electric field integral equation (EFIE), low-frequency breakdown, low-frequency inaccuracy, perturbation method.**

I. Introduction

IT is well-known that the electric field integral equation (EFIE) always suffers from the low-frequency breakdown problem due to the decoupling between the electric field and magnetic field [1]. In the low-frequency regime, the current naturally decomposes itself into a solenoidal (divergence free) part and an irrotational (curl-free) part. This is also known as the Helmholtz decomposition. Both of the two currents are equally important in capturing the inductive and capacitive physics. At low frequencies, the solenoidal current $\boldsymbol{J}_{sol}$ represents eddy currents that produce primarily the magnetic field, whereas the irrotational current $\boldsymbol{J}_{irr}$ represents charge currents that produce primarily the electric field. In the integral representation of EFIE, the electric field is decomposed into the vector potential part and the scalar potential part. They are also phrased as the smoothing term and the hypersingular term. As the frequency approaches zero, the smoothing term is much smaller than the hypersingular term. Due to the finite machine precision, the contribution from the smoothing term will be lost during the numerical process [2]. Moreover, the hypersingular term has a null space because of its divergence operator. It means that, the eigenvalues of the matrix flip-flop between very large values associated with $\boldsymbol{J}_{irr}$ when the hypersingular term dominates, and very small values relevant to $\boldsymbol{J}_{sol}$ when the smoothing term dominates. Hence, the MoM matrix becomes extremely ill-conditioned and converges slowly for the iterative solvers as the mesh density increases [3].

In order to remedy this problem and capture the circuit physics at low frequencies, an idea of the loop-tree or the loop-star decomposition has been proposed to separate the electrostatic and magnetostatic physics [2], [4]–[10]. However, the loop-tree/-star based method is always burdened by the need to search for loops, which is especially difficult for the complicated interconnects which have many entangled long loops. Recently, the Calderón preconditioning (CP) based on the self-regularizing property of the EFIE and Calderón identities has been exploited for preconditioning of the MoM matrix [11]–[13]. Multiplying the EFIE operator $(\mathcal{T})$ by itself provides a well-conditioned second-kind Fredholm integral equation operator. Unfortunately, the direct discretization of $\mathcal{T}^2$ using div-conforming Rao-Wilton-Glisson (RWG) basis function and $\hat{\boldsymbol{n}}_{\boldsymbol{r}} \times$ RWG basis function incurs a singular Gram matrix, where $\hat{\boldsymbol{n}}_{\boldsymbol{r}}$ is a unit normal vector at $\boldsymbol{r}$ on the surface of objects. Alternatively, the composite operator $\mathcal{T}^2$ can be decomposed in terms of its smoothing $(\mathcal{T}_s)$ and hypersingular $(\mathcal{T}_h)$ terms [14]. For closed surfaces, the square of the hypersingular term $(\mathcal{T}_h^2)$ vanishes. In order to discretize the remaining three terms ($\mathcal{T}_s^2$, $\mathcal{T}_h\mathcal{T}_s$, and $\mathcal{T}_s\mathcal{T}_h$), Galerkin method and special intermediate spaces are developed to properly map the range of the first operator onto the domain of the second one. However, it requires calculation of additional matrix elements and has poorer solution accuracy than the original EFIE due to the numerical discretization error. Moreover, applying CP for the open surfaces introduces non-integrable line charges at all edges of the scatterer. The $\mathcal{T}$ operator cannot be projected to the $\mathcal{K}$ operator and the $\mathcal{T}^2$ operator is no longer second kind. Hence, as indicated in [11], [14], the $\mathcal{T}^2$ operator becomes unstable near the discontinuous edges of an open surface, because of the low-order approximation of the effects of edge diffraction.

More recently, a multiplicative form of the Calderón preconditioner (CMP) [15] was developed based on the div- and quasi-curl-conforming basis function, called the Buffa-Christiansen (BC) basis function [16]. This preconditioning is more

Manuscript received November 24, 2011; revised July 08, 2012; accepted August 20, 2012. Date of publication September 20, 2012; date of current version December 28, 2012. This work was supported in part by the Research Grants Council of Hong Kong (GRF 711609 and 716112), in part by the University Grants Council of Hong Kong (Contract No. AoE/P-04/08) and Seed Funding (201111159201).

S. Sun and Z. Ma are with the Department of Electrical and Electronic Engineering, The University of Hong Kong, Hong Kong, China (e-mail: sunsheng@ieee.org; mazuhui@eee.hku.hk).

W. C. Chew is with the Department of Electrical and Computer Engineering, University of Illinois at Urbana-Champaign, Urbana, IL 61801 USA (e-mail: w-chew@uiuc.edu).

Y. G. Liu was with the Department of Electrical and Electronic Engineering, The University of Hong Kong, Hong Kong, China and now with the Institute of Applied Physics and Computational Mathematics, Beijing, China (e-mail: liuyang@lsec.cc.ac.cn).

Color versions of one or more of the figures in this paper are available online at http://ieeexplore.ieee.org.

Digital Object Identifier 10.1109/TAP.2012.2220099

straightforward to implement and easily integrated into existing MoM codes based on RWG basis functions. For the discretization of composite operator $\mathcal{T}^2$, the inner $\mathcal{T}$ operator is discretized by using div-conforming RWG basis function (source) and $\hat{\boldsymbol{n}}_{\boldsymbol{r}} \times$ RWG basis function, while the outer $\mathcal{T}$ operator is discretized by using div- and quasi-curl-conforming BC basis function (source) and $\hat{\boldsymbol{n}}_{\boldsymbol{r}} \times$ BC basis function. Therefore, the resulting Gram matrix is a mixed curl- and quasi-curl-conforming matrix, which is highly sparse and invertible. Subsequently, the CMP is applied on the combined field integral equation (CFIE) formulation for PEC objects [17], and also for the single source integral equations [18]. It should also be noted that the BC basis function represents a subset of the functions proposed by Chen and Wilton in 1990 [19], [21], which was named the dual basis. In other words, the idea of these two basis functions is completely the same. Both of these two basis functions are a linear combination of RWG basis functions on the barycentrically refined triangles within a polygon pair and have the same dual basis property, i.e., approximately orthogonal to the original RWG basis function [20]. Perhaps the reason why the BC basis function has received more attention in the EM community is because of its successful application in the CMP [15], where the well-conditioned nature of the Gram matrices linking the BC basis functions to $\hat{\boldsymbol{n}}_{\boldsymbol{r}} \times$ RWG basis functions is ensured. Hence, we should rightfully call them the Chen-Wilton-Buffa-Christiansen (CWBC) basis function.

As mentioned above, since the composite operator $\mathcal{T}^2$ is a well-conditioned second kind operator, it is immune to low-frequency breakdown and stable at low frequencies, if the $\mathcal{T}_h^2 = 0$ property can be well preserved. However, some literature has shown that the roundoff error of the CMP-EFIE formulation cannot be avoided and causes the preconditioner to fail when the frequency goes to zero [22], [23]. Therefore, the previously developed loop-star decomposition [2] has been further utilized to decouple the electrostatic and magnetostatic fields to overcome this problem. Unfortunately, the Gram matrix is no longer well-conditioned due to the overlapping of the large domain of support of loop and star basis functions.

In other words, the low-frequency breakdown problem cannot be fully avoided in the traditional CMP-EFIE [15]. As also mentioned in [24], the $\mathcal{T}_h^2 = 0$ property has not been well conserved during the direct discretization of the $\mathcal{T}^2$ operator at low frequencies. Therefore, the term $\mathcal{T}_h^2$ must be removed analytically by decomposing $\mathcal{T}^2$ into the remaining three terms. However, we found that there still exists an accuracy problem in this three-term formulation, which will result in a large error in the far-field computation. The same problem also exists in the far-field computations of the magnetic field integral equation (MFIE) at very low frequencies [25]. Because the real-part of the tree current is much smaller than the loop current, the total current error is hard to detect in the MFIE formulation. Although the loop-tree basis function has been used, the zeroth-order loop current still induces a large cancellation during the far-field computation. In addition, the condition number becomes very large because the diagonal-dominant property in the original MFIE operator has been lost after applying the loop-tree basis. To eliminate this error in the tree current detection, perturbation method has been employed, which has been widely used in solving several kinds of physics and engineering problems [26]. As a result, the accurate real part of the tree current has been obtained and the unwanted zeroth-order loop current can be analytically removed. Based on the same strategy of the series expansion, this method has also been utilized in solving the low-frequency inaccuracy of the augmented EFIE [27].

In this paper, we propose the perturbation method to enhance the accuracy of the CMP-EFIE formulation, which transforms the first-kind EFIE operator to the second-kind Fredholm integral equation operator. Without using the loop-tree or the loop-star decomposition, the current distribution can be precisely captured and the error in the far-field computation can also be removed accordingly. Based on the frequency-dependent analysis, the reasons for both low-frequency breakdown and inaccuracy have been given. Numerical examples show that the far-field results can be accurately computed at extremely low frequencies by the proposed perturbation method.

II. Low-Frequency Breakdown

The traditional EFIE operator can be written in its mixed potential form as

$$\mathcal{T}(\boldsymbol{J}) = \mathcal{T}_s(\boldsymbol{J}) + \mathcal{T}_h(\boldsymbol{J}) \tag{1}$$

in which the smoothing ($\mathcal{T}_s$) and hypersingular ($\mathcal{T}_h$) terms are defined as

$$\mathcal{T}_s(\boldsymbol{J}) = i\omega\mu\hat{\boldsymbol{n}}_{\boldsymbol{r}} \times \int_{S'} dS' g(\boldsymbol{r}, \boldsymbol{r}')\boldsymbol{J} \tag{2}$$

$$\mathcal{T}_h(\boldsymbol{J}) = -\frac{1}{i\omega\varepsilon}\hat{\boldsymbol{n}}_{\boldsymbol{r}} \times \nabla \int_{S'} dS' g(\boldsymbol{r}, \boldsymbol{r}')\nabla' \cdot \boldsymbol{J} \tag{3}$$

where

$$g(\boldsymbol{r}, \boldsymbol{r}') = \frac{e^{ik_0|\boldsymbol{r}-\boldsymbol{r}'|}}{4\pi|\boldsymbol{r}-\boldsymbol{r}'|} \tag{4}$$

is the free space Green's function, k_0 is the wave-number in the free space, ε and μ are the relative permeability and permittivity, and $\boldsymbol{J}$ is the surface current on an arbitrarily shaped PEC surface S' whose outward pointing unit normal at $\boldsymbol{r}$ is denoted by $\hat{\boldsymbol{n}}_{\boldsymbol{r}}$.

When $\omega \to 0$, the hypersingular term $\mathcal{T}_h$ which is $O\left(\omega^{-1}\right)$ dominates over the smoothing term $\mathcal{T}_s$ which is $O\left(\omega^{1}\right)$. As mentioned above, because of the existence of the divergence operator in (3) and $\nabla' \cdot \boldsymbol{J}_{sol} = 0$, $\mathcal{T}_h$ has a null space. Thus, the ill-conditioned $\mathcal{T}$ behaves like a first-kind operator between the solenoidal and irrotational subspaces. This makes the impedance matrix nearly singular and unsolvable at low frequencies [2], [4]. This is the so-called low-frequency breakdown problem for the EFIE operator.

In past decades, many research efforts have been carried out to avoid the imbalance inherent in the traditional EFIE operator. The most popular one is the loop-tree or loop-star decomposition, which separates the electrostatic and magnetostatic physics at low frequencies [2], [4], [6]–[10]. In addition, by adding the charge in the unknown list and enforcing the current continuity constraint, the frequency scaling can be normalized in a balanced manner, thus remedying the low-frequency breakdown problem [28]–[30]. However, these methods do not change the

original spectral property of the EFIE operator. The Calderón identity, which can be expressed as [11]–[13]

$$\mathcal{T}^2(\boldsymbol{J}) = -\frac{\boldsymbol{J}}{4} + \mathcal{K}^2(\boldsymbol{J}) \tag{5}$$

can be used to conduct a new operator. In the above, $\mathcal{K}$ is the magnetic field integral equation (MFIE) operator [1]

$$\mathcal{K}(\boldsymbol{J}) = \hat{\boldsymbol{n}}_{\boldsymbol{r}} \times \nabla \times \int_{S'} dS' g(\boldsymbol{r}, \boldsymbol{r}') \boldsymbol{J}. \tag{6}$$

It is important to notice from (5) that the composite operator $\mathcal{T}^2$ is actually a second-kind integral operator with its spectrum accumulated at -0.25. In other words, the $\mathcal{T}$ operator can be directly utilized to precondition itself, which is so-called "self-regularizing property" of the $\mathcal{T}$ operator.

According to the decomposition in (1), the composite operator $\mathcal{T}^2$ can be further expanded as

$$\mathcal{T}^2 = \mathcal{T}_s^2 + \mathcal{T}_s\mathcal{T}_h + \mathcal{T}_h\mathcal{T}_s + \mathcal{T}_h^2 \tag{7}$$

where

$$\mathcal{T}_s^2(\boldsymbol{J}) = -\omega^2\mu^2 \hat{\boldsymbol{n}}_{\boldsymbol{r}} \times \int_{S'} dS' g(\boldsymbol{r}, \boldsymbol{r}') \times \left[\hat{\boldsymbol{n}}'_{\boldsymbol{r}} \times \int_{S''} dS'' g(\boldsymbol{r}', \boldsymbol{r}'') \boldsymbol{J}\right] \tag{8}$$

$$\mathcal{T}_s\mathcal{T}_h(\boldsymbol{J}) = -\hat{\boldsymbol{n}}_{\boldsymbol{r}} \times \int_{S'} dS' g(\boldsymbol{r}, \boldsymbol{r}') \times \left[\hat{\boldsymbol{n}}'_{\boldsymbol{r}} \times \nabla' \int_{S''} dS'' g(\boldsymbol{r}', \boldsymbol{r}'') \nabla'' \cdot \boldsymbol{J}\right] \tag{9}$$

$$\mathcal{T}_h\mathcal{T}_s(\boldsymbol{J}) = -\hat{\boldsymbol{n}}_{\boldsymbol{r}} \times \nabla \int_{S'} dS' g(\boldsymbol{r}, \boldsymbol{r}') \nabla' \cdot \left[\hat{\boldsymbol{n}}'_{\boldsymbol{r}} \times \int_{S''} dS'' g(\boldsymbol{r}', \boldsymbol{r}'') \boldsymbol{J}\right] \tag{10}$$

$$\mathcal{T}_h^2(\boldsymbol{J}) = -\frac{1}{\omega^2\varepsilon^2} \hat{\boldsymbol{n}}_{\boldsymbol{r}} \times \nabla \int_{S'} dS' g(\boldsymbol{r}, \boldsymbol{r}') \nabla' \cdot \left[\hat{\boldsymbol{n}}'_{\boldsymbol{r}} \times \nabla' \int_{S''} dS'' g(\boldsymbol{r}', \boldsymbol{r}'') \nabla'' \cdot \boldsymbol{J}\right]. \tag{11}$$

Recalling the surface Helmholtz decomposition of the surface current $\boldsymbol{J}$ [31], [32]

$$\boldsymbol{J} = \nabla_S \phi + \hat{\boldsymbol{n}}_{\boldsymbol{r}} \times \nabla_S \psi \tag{12}$$

where ϕ and ψ are scalar functions defined on S. The first term of (12) is purely irrotational (curl-free) while the second term is purely solenoidal (divergence-free). It is easy to show that [11]

$$\nabla_S \cdot (\mathcal{T}_h(\boldsymbol{J})) = \nabla_S \cdot (\hat{\boldsymbol{n}}_{\boldsymbol{r}} \times \nabla\Phi) = 0. \tag{13}$$

As a result, the square of the hypersingular term ($\mathcal{T}_h^2$) in (11) is identically zero. Consequently, the decomposed operator $\mathcal{T}^2$ in (7) can be re-written as

$$\mathcal{T}^2 = \mathcal{T}_s^2 + \mathcal{T}_h\mathcal{T}_s + \mathcal{T}_s\mathcal{T}_h. \tag{14}$$

Notice that from (8) to (10), the $\mathcal{T}_s^2 \sim O(\omega^2)$, while the $\mathcal{T}_s\mathcal{T}_h + \mathcal{T}_h\mathcal{T}_s \sim O(\omega^0)$, when $\omega \to 0$. In other words, the $\mathcal{T}_s\mathcal{T}_h$ and $\mathcal{T}_h\mathcal{T}_s$ are frequency invariant, so that the two terms behave like an identity operator. Meanwhile, $\mathcal{T}_s^2$ behaves like a compact operator, and approaches zero when $\omega \to 0$. Therefore, the total operator $\mathcal{T}^2$ can be considered as an identity operator plus a compact operator, which makes it a well-conditioned second-kind Fredholm integral operator and immune to low-frequency breakdown. Meanwhile, $\mathcal{T}_h^2 \sim O(\omega^{-2})$. It implies that the square of the hypersingular term has to be set to zero; otherwise it will swamp the contributions from the other three terms at low frequencies. However, if $\boldsymbol{J}$ is of the order smaller than ω^0 and higher order current is also important for certain problems, the decomposed $\mathcal{T}^2$ (without $\mathcal{T}_h^2$) still decreases with frequency. It does not cause the breakdown of the MoM, but causes the inaccuracy of the electric current at low frequencies, which will be discussed in the next section.

III. Low-Frequency Inaccuracy

In this work, we directly discretize the inner and outer $\mathcal{T}$ operator for the $\mathcal{T}^2$ operator by using the dual finite element space. To avoid the low-frequency breakdown problem, the decomposed operator with remaining three terms in (14) will be used in the following discretization procedure. By following the same strategy of the discretization using the aforementioned CWBC basis function [16], [19], the decomposed $\mathcal{T}^2$ operator can be discretized as

$$\left(\mathcal{T}^2\right)_{\text{dis}} = k_0^2 \overline{\boldsymbol{Z}}^s_{CWBC} \overline{\boldsymbol{G}}_m^{-1} \overline{\boldsymbol{Z}}^s_{RWG} + \overline{\boldsymbol{Z}}^h_{CWBC} \overline{\boldsymbol{G}}_m^{-1} \overline{\boldsymbol{Z}}^s_{RWG} + \overline{\boldsymbol{Z}}^s_{CWBC} \overline{\boldsymbol{G}}_m^{-1} \overline{\boldsymbol{Z}}^h_{RWG} \tag{15}$$

where

$$\left[\overline{\boldsymbol{Z}}^q_p\right]_{m,n} = \langle \hat{\boldsymbol{n}}_{\boldsymbol{r}} \times \boldsymbol{f}_{pm},\ \mathcal{T}_q(\boldsymbol{f}_{pn}) \rangle \tag{16}$$

is the impedance matrix obtained by using CWBC or RWG basis function with the notation of the subscript p, the superscript q indicates the smoothing (s) or hypersingular (h) term, and

$$\left[\overline{\boldsymbol{G}}_m\right]_{m,n} = \langle \hat{\boldsymbol{n}}_{\boldsymbol{r}} \times \boldsymbol{f}_{RWGm},\ \boldsymbol{f}_{CWBCn} \rangle \tag{17}$$

is the Gram matrix linking the range and domain spaces. Then, we can write the CMP-EFIE matrix system as

$$k_0^2 \overline{\boldsymbol{Z}}^s_{CWBC} \overline{\boldsymbol{G}}_m^{-1} \overline{\boldsymbol{Z}}^s_{RWG} \boldsymbol{I}_{RWG} + \overline{\boldsymbol{Z}}^h_{CWBC} \overline{\boldsymbol{G}}_m^{-1} \overline{\boldsymbol{Z}}^s_{RWG} \boldsymbol{I}_{RWG} + \overline{\boldsymbol{Z}}^s_{CWBC} \overline{\boldsymbol{G}}_m^{-1} \overline{\boldsymbol{Z}}^h_{RWG} \boldsymbol{I}_{RWG} = ik_0 \overline{\boldsymbol{Z}}^s_{CWBC} \overline{\boldsymbol{G}}_m^{-1} \boldsymbol{V}_{RWG} + \frac{1}{ik_0} \overline{\boldsymbol{Z}}^h_{CWBC} \overline{\boldsymbol{G}}_m^{-1} \boldsymbol{V}_{RWG} \tag{18}$$

where $\boldsymbol{I}_{RWG}$ denotes the unknown vector of electric current and $\boldsymbol{V}_{RWG}$ is the known excitation vector due to the incident field.

At very low frequencies, the scalar Green's function in (4) is well approximated as

$$g(\boldsymbol{r}, \boldsymbol{r}') \approx \frac{1}{4\pi R}\left[1 + ik_0 R + \frac{1}{2}(ik_0 R)^2\right] \tag{19}$$

where $R = |\boldsymbol{r} - \boldsymbol{r}'|$ and $|ik_0 R| \ll 1$. We notice that when $k_0 \to 0$, the leading terms of the Green's function in (19) are the first two terms. Thus, the real part of g is of order of ω^0, while the imaginary part of g is of order ω^1. Since the testing and basis functions in (18) are frequency invariant, the impedance

matrices and the excitation vector are on the same order of the Green's function. Subsequently, the frequency dependence of each term in (18) for a plane wave scattering problem can be easily estimated as

$$\left[\overline{\boldsymbol{Z}}^{ss}\left(\omega^2,\omega^3\right)+\overline{\boldsymbol{Z}}^{hs}\left(\omega^0,\omega^1\right)+\overline{\boldsymbol{Z}}^{sh}\left(\omega^0,\omega^1\right)\right]\cdot\boldsymbol{I}\left(\omega^a,\omega^b\right)=\overline{\boldsymbol{Z}}^{s}\boldsymbol{V}\left(\omega^2,\omega^1\right)+\overline{\boldsymbol{Z}}^{h}\boldsymbol{V}\left(\omega^0,\omega^{-1}\right). \quad (20)$$

Matching the real and imaginary parts of the two sides of (20) yields

$$a\geq 0,\quad b\geq -1. \quad (21)$$

That means in CMP-EFIE, the real part of $\boldsymbol{I}$ is on the order of ω^0, and the imaginary part of $\boldsymbol{I}$ is on the order of ω^{-1}. However, as shown in [25], [27], the frequency dependence of the currents for the loop-tree decomposition is given by

$$\boldsymbol{I}_L\left(\omega^0,\omega^1\right),\ \boldsymbol{I}_C\left(\omega^2,\omega^1\right). \quad (22)$$

At low frequencies, the leading term of current is loop current which is $O(\omega^0)$, while the imaginary part of the current which is $O(\omega^1)$ has the mixed contribution from both loop and tree currents. This implies that, the imaginary part of the current in (22) should be on the order of ω^1, that is $b\geq 1$, which is a subset of $b\geq -1$ obtained by (20). In other words, it is difficult to obtain the accurate imaginary part of the current at low frequencies by solving CMP-EFIE directly, due to the finite machine precision. This is the reason for the low-frequency inaccuracy of the CMP-EFIE operator.

IV. Perturbation Method for CMP-EFIE

In order to remedy the aforementioned low-frequency inaccuracy problem, a perturbation method is employed in this section [25]–[27]. Following the expansion of the Green's function in (19), the sub-matrices in (16) can be expanded with respect to a small parameter $\delta=ik_0$. Then, we have

$$\left[\overline{\boldsymbol{Z}}_p^{q}\right]=\left[\overline{\boldsymbol{Z}}_p^{q(0)}\right]+\delta\left[\overline{\boldsymbol{Z}}_p^{q(1)}\right]+\delta^2\left[\overline{\boldsymbol{Z}}_p^{q(2)}\right]+O(\delta^3) \quad (23)$$

where the impedance matrices for the smoothing term are given by

$$\left[\overline{\boldsymbol{Z}}_p^{s(0)}\right]_{mn}=\frac{\mu}{4\pi}\int_{S_m}dS\boldsymbol{f}_{pm}(\boldsymbol{r})\cdot\int_{S_n}dS'\frac{1}{|\boldsymbol{r}-\boldsymbol{r}'|}\boldsymbol{f}_{pn}(\boldsymbol{r}') \quad (24)$$

$$\left[\overline{\boldsymbol{Z}}_p^{s(1)}\right]_{mn}=\frac{\mu}{4\pi}\int_{S_m}dS\boldsymbol{f}_{pm}(\boldsymbol{r})\cdot\int_{S_n}dS'\boldsymbol{f}_{pn}(\boldsymbol{r}') \quad (25)$$

$$\left[\overline{\boldsymbol{Z}}_p^{s(2)}\right]_{mn}=\frac{\mu}{8\pi}\int_{S_m}dS\boldsymbol{f}_{pm}(\boldsymbol{r})\cdot\int_{S_n}dS'|\boldsymbol{r}-\boldsymbol{r}'|\,\boldsymbol{f}_{pn}(\boldsymbol{r}') \quad (26)$$

and the impedance matrices for the hypersingular term are given by

$$\left[\overline{\boldsymbol{Z}}_p^{h(0)}\right]_{mn}=\frac{1}{4\pi\varepsilon}\nabla\int_{S_m}dS\boldsymbol{f}_{pm}(\boldsymbol{r})\cdot\int_{S_n}dS'\frac{1}{|\boldsymbol{r}-\boldsymbol{r}'|}\nabla'\cdot\boldsymbol{f}_{pn}(\boldsymbol{r}') \quad (27)$$

$$\left[\overline{\boldsymbol{Z}}_p^{h(1)}\right]_{mn}=\frac{1}{4\pi\varepsilon}\nabla\int_{S_m}dS\boldsymbol{f}_{pm}(\boldsymbol{r})\cdot\int_{S_n}dS'\nabla'\cdot\boldsymbol{f}_{pn}(\boldsymbol{r}') \quad (28)$$

$$\left[\overline{\boldsymbol{Z}}_p^{h(2)}\right]_{mn}=\frac{1}{8\pi\varepsilon}\nabla\int_{S_m}dS\boldsymbol{f}_{pm}(\boldsymbol{r})\cdot\int_{S_n}dS'|\boldsymbol{r}-\boldsymbol{r}'|\,\nabla'\cdot\boldsymbol{f}_{pn}(\boldsymbol{r}'). \quad (29)$$

At low frequencies, $\overline{\boldsymbol{Z}}_p^{q}\approx\overline{\boldsymbol{Z}}_p^{q(0)}$, because the zeroth-order of the Green's function in (19) is equal to its original form of (4) in static regime.

For the current and excitation vectors, we use the same notations as those in [27] as

$$ik_0\boldsymbol{j}=\boldsymbol{j}^{(0)}+\delta\boldsymbol{j}^{(1)}+\delta^2\boldsymbol{j}^{(2)}+O(\delta^3) \quad (30)$$

$$\boldsymbol{b}=\boldsymbol{b}^{(0)}+\delta\boldsymbol{b}^{(1)}+\delta^2\boldsymbol{b}^{(2)}+O(\delta^3) \quad (31)$$

where

$$\left[\boldsymbol{b}^{(0)}\right]_m=-\eta^{-1}\int_{S_m}dS\boldsymbol{f}_{RWGm}(r)\cdot\boldsymbol{E}_0 \quad (32)$$

$$\left[\boldsymbol{b}^{(1)}\right]_m=-\eta^{-1}\int_{S_m}dS\boldsymbol{f}_{RWGm}(r)\cdot\boldsymbol{E}_0\left(\hat{k}_{inc}\cdot\tilde{\boldsymbol{r}}\right) \quad (33)$$

$$\left[\boldsymbol{b}^{(2)}\right]_m=-\frac{1}{2}\eta^{-1}\int_{S_m}dS\boldsymbol{f}_{RWGm}(r)\cdot\boldsymbol{E}_0\left(\hat{k}_{inc}\cdot\tilde{\boldsymbol{r}}\right)^2 \quad (34)$$

and $\hat{k}_{inc}$ is the unit vector of the incident direction and the tilde above $\boldsymbol{r}$ indicates the normalization by l, where l is a typical length scale.

Substituting them into (18) and matching the coefficients of like powers of δ, we obtain a recurrent system of equations for the current functions $\boldsymbol{j}$. Firstly, matching the zeroth order of δ gives the lowest order equation as

$$\left[\overline{\boldsymbol{Z}}_{CWBC}^{s(0)}\overline{\boldsymbol{G}}_m^{-1}\overline{\boldsymbol{Z}}_{RWG}^{h(0)}+\overline{\boldsymbol{Z}}_{CWBC}^{h(0)}\overline{\boldsymbol{G}}_m^{-1}\overline{\boldsymbol{Z}}_{RWG}^{s(0)}\right]\cdot\boldsymbol{j}^{(0)}=\overline{\boldsymbol{Z}}_{CWBC}^{h(0)}\overline{\boldsymbol{G}}_m^{-1}\boldsymbol{b}^{(0)}. \quad (35)$$

We notice that the impedance matrix is equal to the three-term CMP-EFIE without $\mathcal{T}_h^2$ in (14) in static regime, where the contributions from the $\mathcal{T}_s^2$ at $O(\omega^2)$ disappear. That means the resultant matrix is in the form formulated by an identity operator plus a compact operator as the aforementioned analysis. Hence,

it has a good spectral property at low frequencies and is easy to see the convergence of an iterative solver.

Then, the first-order equation can be obtained by matching the first order of δ as

$$\begin{aligned}&\left[\overline{\boldsymbol{Z}}^{s(0)}_{CWBC}\overline{\boldsymbol{G}}_m^{-1}\overline{\boldsymbol{Z}}^{h(0)}_{RWG}+\overline{\boldsymbol{Z}}^{h(0)}_{CWBC}\overline{\boldsymbol{G}}_m^{-1}\overline{\boldsymbol{Z}}^{s(0)}_{RWG}\right]\cdot\boldsymbol{j}^{(1)}\\&\quad=\overline{\boldsymbol{Z}}^{h(1)}_{CWBC}\overline{\boldsymbol{G}}_m^{-1}\boldsymbol{b}^{(0)}+\overline{\boldsymbol{Z}}^{h(0)}_{CWBC}\overline{\boldsymbol{G}}_m^{-1}\boldsymbol{b}^{(1)}\\&\qquad-\left[\overline{\boldsymbol{Z}}^{s(1)}_{CWBC}\overline{\boldsymbol{G}}_m^{-1}\overline{\boldsymbol{Z}}^{h(0)}_{RWG}+\overline{\boldsymbol{Z}}^{h(1)}_{CWBC}\overline{\boldsymbol{G}}_m^{-1}\overline{\boldsymbol{Z}}^{s(0)}_{RWG}\right]\cdot\boldsymbol{j}^{(0)}\\&\qquad-\left[\overline{\boldsymbol{Z}}^{s(0)}_{CWBC}\overline{\boldsymbol{G}}_m^{-1}\overline{\boldsymbol{Z}}^{h(1)}_{RWG}+\overline{\boldsymbol{Z}}^{h(0)}_{CWBC}\overline{\boldsymbol{G}}_m^{-1}\overline{\boldsymbol{Z}}^{s(1)}_{RWG}\right]\\&\qquad\cdot\boldsymbol{j}^{(0)}.\end{aligned}\tag{36}$$

With the zeroth-order current, we can solve for the first order of them by inverting the same impedance matrix. During the updating of the right hand side vector, only the contributions from the first order $\mathcal{T}_s\mathcal{T}_h$ and $\mathcal{T}_h\mathcal{T}_s$ operators are iterated.

Next, the second order equation can also be invoked

$$\begin{aligned}&\left[\overline{\boldsymbol{Z}}^{s(0)}_{CWBC}\overline{\boldsymbol{G}}_m^{-1}\overline{\boldsymbol{Z}}^{h(0)}_{RWG}+\overline{\boldsymbol{Z}}^{h(0)}_{CWBC}\overline{\boldsymbol{G}}_m^{-1}\overline{\boldsymbol{Z}}^{s(0)}_{RWG}\right]\cdot\boldsymbol{j}^{(2)}\\&\quad=\overline{\boldsymbol{Z}}^{s(0)}_{CWBC}\overline{\boldsymbol{G}}_m^{-1}\boldsymbol{b}^{(0)}+\overline{\boldsymbol{Z}}^{h(1)}_{CWBC}\overline{\boldsymbol{G}}_m^{-1}\boldsymbol{b}^{(1)}+\overline{\boldsymbol{Z}}^{h(0)}_{CWBC}\overline{\boldsymbol{G}}_m^{-1}\boldsymbol{b}^{(2)}\\&\qquad-\left[\overline{\boldsymbol{Z}}^{s(0)}_{CWBC}\overline{\boldsymbol{G}}_m^{-1}\overline{\boldsymbol{Z}}^{h(1)}_{RWG}+\overline{\boldsymbol{Z}}^{h(0)}_{CWBC}\overline{\boldsymbol{G}}_m^{-1}\overline{\boldsymbol{Z}}^{s(1)}_{RWG}\right]\cdot\boldsymbol{j}^{(1)}\\&\qquad-\left[\overline{\boldsymbol{Z}}^{s(1)}_{CWBC}\overline{\boldsymbol{G}}_m^{-1}\overline{\boldsymbol{Z}}^{h(0)}_{RWG}+\overline{\boldsymbol{Z}}^{h(1)}_{CWBC}\overline{\boldsymbol{G}}_m^{-1}\overline{\boldsymbol{Z}}^{s(0)}_{RWG}\right]\cdot\boldsymbol{j}^{(1)}\\&\qquad-\left[\overline{\boldsymbol{Z}}^{s(0)}_{CWBC}\overline{\boldsymbol{G}}_m^{-1}\overline{\boldsymbol{Z}}^{s(0)}_{RWG}\right]\cdot\boldsymbol{j}^{(0)}\\&\qquad-\left[\overline{\boldsymbol{Z}}^{s(1)}_{CWBC}\overline{\boldsymbol{G}}_m^{-1}\overline{\boldsymbol{Z}}^{h(1)}_{RWG}+\overline{\boldsymbol{Z}}^{h(1)}_{CWBC}\overline{\boldsymbol{G}}_m^{-1}\overline{\boldsymbol{Z}}^{s(1)}_{RWG}\right]\cdot\boldsymbol{j}^{(0)}\\&\qquad-\left[\overline{\boldsymbol{Z}}^{s(0)}_{CWBC}\overline{\boldsymbol{G}}_m^{-1}\overline{\boldsymbol{Z}}^{h(2)}_{RWG}+\overline{\boldsymbol{Z}}^{h(0)}_{CWBC}\overline{\boldsymbol{G}}_m^{-1}\overline{\boldsymbol{Z}}^{s(2)}_{RWG}\right]\cdot\boldsymbol{j}^{(0)}\\&\qquad-\left[\overline{\boldsymbol{Z}}^{s(2)}_{CWBC}\overline{\boldsymbol{G}}_m^{-1}\overline{\boldsymbol{Z}}^{h(0)}_{RWG}+\overline{\boldsymbol{Z}}^{h(2)}_{CWBC}\overline{\boldsymbol{G}}_m^{-1}\overline{\boldsymbol{Z}}^{s(0)}_{RWG}\right]\cdot\boldsymbol{j}^{(0)}.\end{aligned}\tag{37}$$

Once the currents at the first three orders are obtained by solving (35)–(37), the far-field results at very low frequencies can be obtained accurately.

It is important to notice that the impedance matrices at the left-hand side of (35)–(37) have both contributions from the smoothing and hypersingular terms, thus avoiding the null space problem and breakdown at low frequencies. Similar to the augmented EFIE formulations [27], the decomposed CMP-EFIE operator is balanced at low frequencies after setting $\mathcal{T}_h^2 = 0$. As mentioned above, the contribution from the last term $\mathcal{T}_h^2$ in (7) is of $O(\omega^{-2})$, which is much lager than the contributions from the other three terms. Consequently, the first three terms are diminishing as frequency decreases, so that the whole matrix system breaks down because of solving a non-existent term, that is, $\mathcal{T}_h^2 \equiv 0$.

In particular, we can observe from (22) that the leading term of current $\boldsymbol{j}$ is on the order of ω^0 for plane wave scattering problems. It implies that the leading term of $ik_0\boldsymbol{j}$ is on the order of ω^1. Hence, the zeroth order current $\boldsymbol{j}^{(0)}$ in (30), which is on the order of ω^0, should be zero. By utilizing this natural characteristic, the solution complexity of the matrix systems in (35)–(37) can be reduced significantly.

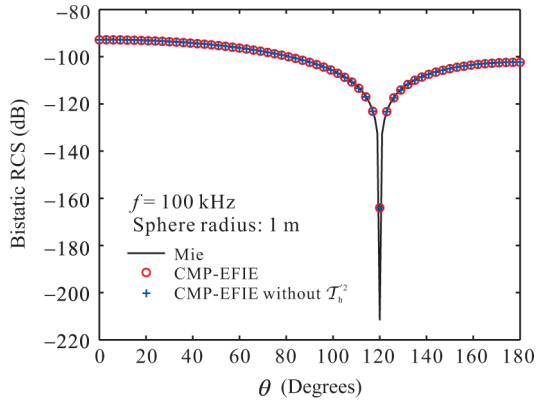

Fig. 1. Comparison of the bistatic RCS of a PEC sphere for the vertical polarization. The radius of the PEC sphere is 1 m and the frequency is 100 kHz.

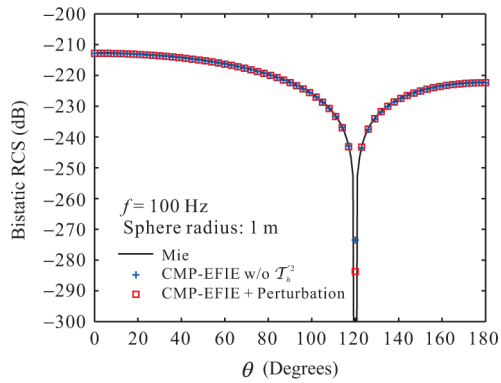

Fig. 2. Comparison of the bistatic RCS of a PEC sphere for the vertical polarization. The radius of the PEC sphere is 1 m and the frequency is 100 Hz.

V. Numerical Examples

Different from the previous solutions using loop-star decomposition [22], [23], the proposed CMP-EFIE with the perturbation method keeps the sparse characteristic of the Gram matrix. Without the need for loop search, the enhanced CMP-EFIE successfully remedies the inaccuracy problem at low frequencies.

Fig. 1 shows the comparison between Mie series, traditional CMP-EFIE ($\mathcal{T}^2$) and the decomposed CMP-EFIE without $\mathcal{T}_h^2$ at 100 kHz. In this numerical example, an x-polarized plane wave impinges onto a PEC sphere from the $+z$ direction. The sphere centers at the origin and has a radius of 1 m. We discretize the surface into 578 triangular patches, equivalent to 867 inner edges. From the results, we find that both the two CMP-EFIE methods have no breakdown or inaccuracy problem, since the frequency is not very low. Then, we did the comparison at 100 Hz, as shown in Fig. 2. The traditional CMP-EFIE cannot converge due to the low-frequency breakdown as discussed in Section II. With the perturbation method, the decomposed CMP-EFIE gives the right results, while the decomposed CMP-EFIE without perturbation method is still able to deliver correct results. However, when the frequency becomes even lower, the situation worsens. The decomposed CMP-EFIE without perturbation method does not have convergent problem, but incurs an inaccuracy problem. As shown in Fig. 3, at 1 Hz, the decomposed CMP-EFIE is wrong due to the low-frequency inaccuracy of electric current, while the

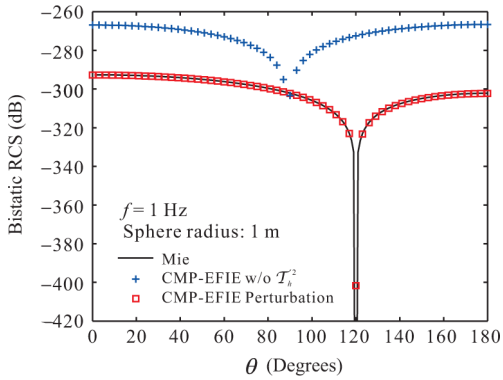

Fig. 3. Comparison of the bistatic RCS of a PEC sphere for the vertical polarization. The radius of the PEC sphere is 1 m and the frequency is 1 Hz.

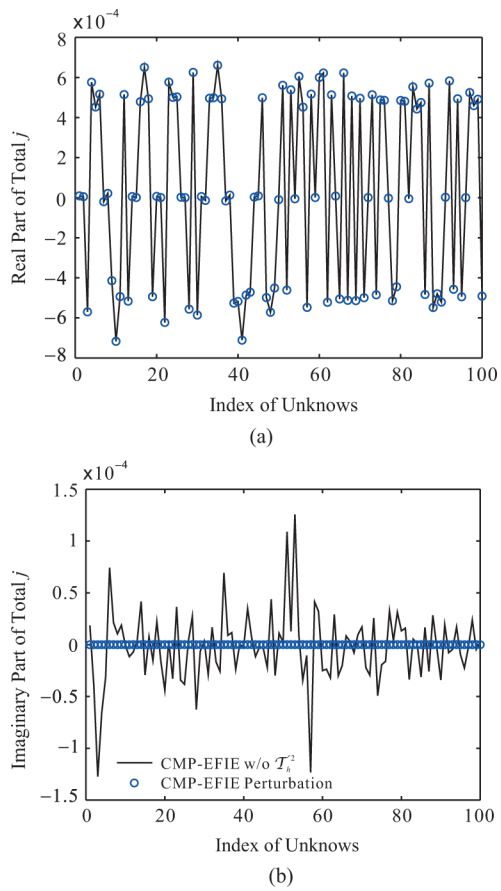

Fig. 4. The comparison of total calculated $\boldsymbol{j}$ using the decomposed CMP-EFIE without/with the perturbation method. (a) Real part. (b) Imaginary part. The radius of the PEC sphere is 1 m and the frequency is 1 Hz.

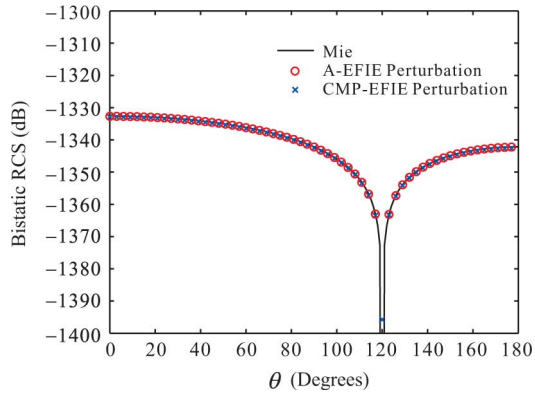

Fig. 5. Comparison of the bistatic RCS of a PEC sphere for the vertical polarization. The radius of the PEC sphere is 1 m and the frequency is 10^{-26} Hz.

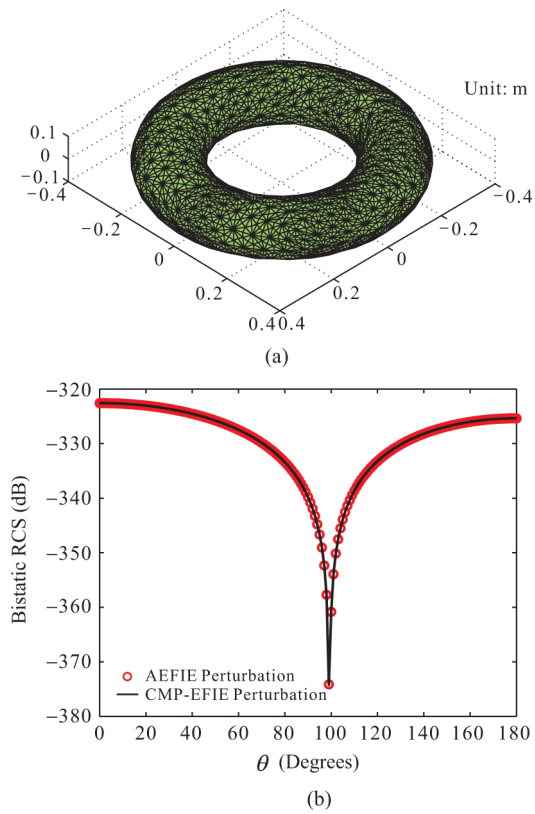

Fig. 6. (a) Geometry of a PEC torus (b) Comparison of the bistatic RCS for the vertical polarization at 1 Hz.

one with the perturbation method shows good accuracy in comparison with the results obtained from Mie series. The aforementioned frequency dependence analysis shows that, this inaccuracy problem is due to the difficulty in obtaining the accurate imaginary part of total electric current. As shown in Figs. 4(a) and 4(b), although double precision has been used, the error in the imaginary part of $\boldsymbol{j}$ is still involved without perturbation method, while its real part has a good agreement with the one obtained by the perturbation method. As our previous analysis shows (also discussed in [27]), both of the loop and tree currents at different orders are equally important for the far-field computations at very low frequencies, which are equivalent to a magnetic dipole and an electric dipole, respectively, according to Rayleigh scattering theory.

Then, we did the comparison at an extremely low frequency, 10^{-26} Hz, as shown in Fig. 5. It is clear that the bistatic RCS computed by the decomposed CMP-EFIE with the perturbation method has an excellent agreement with the results obtained from Mie series and A-EFIE with the perturbation method [27].

Futhermore, we replace the sphere with a PEC torus shown in Fig. 6(a), which has two global loops. The radius of the tube is 0.1 m and the distance from the center of the tube to the center

TABLE I
COMPUTATIONAL COMPLEXITY AND ITERATION NUMBERS OF NUMERICAL EXAMPLES.

Methods	Computational Complexity	Iteration Numbers N_{it} (GMRES-30 and Tolerance: 1×10^{-7})					
		Fig.1:Sphere @100KHz	Fig.2:Sphere @100Hz	Fig.3:Sphere @1Hz	Fig.5:Sphere @10^{-26}Hz	Fig.6:Torus @1Hz	Fig.7:Flying saucer @10^{-9}Hz
AEFIE [30]	$N_{it}(C_Z(N+P))$	28	32	/	/	/	/
AEFIE + Perturbation [27]	$2N_{order}N_{it}(C_Z(N+P))$	35	35	35	35	42	38
CMP-EFIE [15]	$N_{it}^{CMP}(2C_Z(N)+O(N))$	9	/	/	/	/	/
CMP-EFIE w/o $\mathcal{T}_h^2$ [24]	$3N_{it}^{CMP}(2C_Z(N)+O(N))$	9	9	/	/	/	/
CMP-EFIE + Perturbation	$2N_{order}N_{it}^{CMP}(2C_Z(N)+O(N))$	9	9	9	9	11	15

C_Z: the cost of matrix-vector product in the standard matrix system; N: the number of edge current unknowns; P: the number of charge unknowns;
N_{it} and N_{it}^{CMP}: the number of iterations to achieve the convergence without/with using the CMP;
N_{order}: the number of orders in perturbation method.

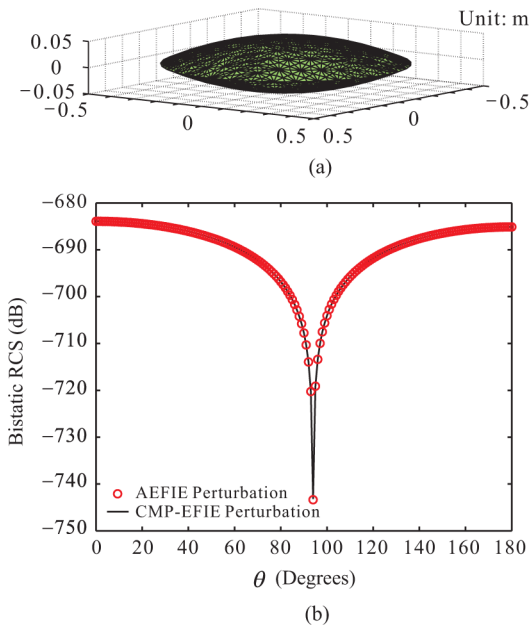

Fig. 7. (a) Geometry of a PEC flying saucer (b) Comparison of the bistatic RCS for the vertical polarization at 10^{-9} Hz.

of the torus is 0.3 m. We discretize the surface into 1,066 triangular patches, equivalent to 1,599 inner edges. Fig. 6(b) shows the comparison of RCS between A-EFIE [27] and the decomposed CMP-EFIE with the perturbation method at 1 Hz. Similar to the sphere case, the decomposed CMP-EFIE with the perturbation method generates correct results as A-EFIE with the perturbation method does. However, following the study in [33], the magnetostatic nullspace for torus structure still exists in the CMP-EFIE with the perturbation method, which is strictly a near field phenomenon. Although its contribution in the far-field computation is trivial, the condition number of system matrix becomes higher due to this nullspace. Hence, the additional diagonally preconditioning Gram matrix [15] is preferred to further improve the convergence. As discussed in [34], to ensure the near field accuracy, the magnetic field generated by the surface current and the excitation must be zero just inside the boundary of the torus. It implies that if the current in the magnetostatic nullspace is not excited by the source, a well-behaved solution current may still be possible. This low-frequency behavior has been well addressed in [34], where the testing functions can be thought of as being slightly inside the boundary while the basis functions are on the boundary.

The third example is a PEC flying saucer with a sharp edge, as shown in Fig. 7. The thickness of the flying saucer is 0.1 m and the radius of its curvature is 2 m. We discretize the surface into 526 triangular patches, equivalent to 789 inner edges, which is corresponding to 3156 barycentrically refined triangle patches and 4734 refined inner edges. Fig. 7(a) shows the comparison of RCS between A-EFIE [27] and the decomposed CMP-EFIE with the perturbation method at 10^{-9} Hz. Without perturbation method, the decomposed CMP-EFIE loses accuracy, while the decomposed CMP-EFIE with the perturbation method delivers accurate results down to DC.

Since the impedance matrices at different orders have to be calculated and stored, the overall computational cost of the perturbation method could be higher than the traditional CMP-based methods. Table I compares the computational cost and the iteration numbers with other methods for the above numerical examples. C_Z is the cost of matrix-vector product in the original matrix system, while N and P indicate the number of current and charge unknowns, respectively. N_{it} and N_{it}^{CMP} are the number of iterations to achieve the convergence without/with using the CMP. Here, N_{order} is the number of orders involved in perturbation method. Note that only the impedance matrices at the zeroth order are involved in the iterative process. It means that the computational cost of the CMP-EFIE will be doubled after using perturbation method at each order. However, the well-behaved solution can be undoubtedly achieved at extremely low frequencies and the iteration numbers for the CMP-based methods are much smaller than the other methods.

VI. CONCLUSION

In this paper, we have proposed the perturbation method for the low-frequency problems in the CMP-EFIE. Both of the low-frequency breakdown and inaccuracy problems have been well addressed. Due to the null space of the square of the hypersingular term, the low-frequency breakdown problem cannot be avoided in the CMP-EFIE. By removing the last term from the decomposed $\mathcal{T}^2$ operator, the remaining three terms are in the form of an identity operator plus a compact operator, making

it the second-kind integral operator which is very stable at low frequencies. Although the computational cost is increased, the resultant impedance matrices are well-conditioned and easy to converge in an iterative solver. However, it still has an inaccuracy problem, because of the machine precision in calculating the imaginary part of the low-frequency electric current. By using a perturbation method, the accurate imaginary part of total electric current has been obtained. Numerical examples show that the far-field results can be computed accurately at extremely low frequencies.

Appendix
Accuracy Estimate of the Perturbation Method

To simplify the formulation during the perturbation process, the second-order approximation has been used as

$$g(\boldsymbol{r},\boldsymbol{r}') \approx \frac{1}{4\pi R}\left[1 + ik_0R + \frac{1}{2!}(ik_0R)^2 + O((ik_0R)^3)\right] \tag{38}$$

where any orders above $(ik_0R)^2$ has been ignored under the assumption of $|ik_0R| \ll 1$. That means when $|ik_0R|$ approaches 1, the above approximation will lose the accuracy. For example, we consider the case in Fig. 1 with a unit PEC sphere. When $f = 0.01$ GHz, $|ik_0R_{\max}| = 0.4189$, we have

$$g(\boldsymbol{r},\boldsymbol{r}') = 0.0397\dot{9} + i0.0166\dot{7} - 0.0034\dot{9} - i0.000487\dot{7} + 0.00005104\dot{} + \cdots \tag{39}$$

The addition of all subsequent terms from 4th term will not affect the third decimal place (3 d.p.). Also, when $f = 0.001$ GHz, $|ik_0R_{\max}| = 0.04189$, we have

$$g(\boldsymbol{r},\boldsymbol{r}') = 0.0397\dot{9} + i0.00166\dot{7} - 0.000034\dot{9} - i0.000000487\dot{7} + 0.000000005104\dot{} + \cdots \tag{40}$$

Hence the value to 6 d.p. can be found for the second-order approximation. Obviously, the series converges with the remaining term goes to zero. Therefore, in order to achieve the desired accuracy to 7 d.p, in this example, the frequency can be estimated by

$$\frac{1}{3!}(ik_0R)^3 < 10^{-7} \Rightarrow f < 0.20\dot{} \text{ MHz}. \tag{41}$$

Acknowledgment

The authors would like to thank anonymous reviewers for improving this work with their helpful comments and suggestions, and Prof. M. Tong, Tongji University, China, Q. S. Liu and Dr. Y. H. Lo, The University of Hong Kong, Hong Kong, for their valuable discussion and suggestions in this work.

References

[1] W. C. Chew, M. S. Tong, and B. Hu, *Integral Equation Methods for Electromagnetic and Elastic Waves*. San Rafael, CA: Morgan & Claypool, 2008.

[2] J. S. Zhao and W. C. Chew, "Integral equation solution of maxwell's equations from zero frequency to microwave frequency," *IEEE Trans. Antennas Propag.*, vol. 48, no. 10, pp. 1635–1645, Oct. 2000.

[3] F. Vipiana, P. Pirinoli, and G. Vecchi, "Spectral properties of the EFIE-MOM matrix for dense meshes with different type of bases," *IEEE Trans. Antennas Propag.*, vol. 55, no. 11, pp. 3229–3238, Nov. 2007.

[4] D. R. Wilton and A. W. Glisson, "On improving the stability of the electric field integral equation at low frequencies," in *Proc. URSI Radio Sci. Meeting*, Los Angeles, CA, Jun. 1981, p. 24.

[5] J. R. Mautz and R. F. Harrington, "An E-field solution for a conducting surface small or comparable to the wavelength," *IEEE Trans. Antennas Propag.*, vol. 32, no. 4, pp. 330–339, Apr. 1984.

[6] M. Burton and S. Kashyap, "A study of a recent moment-method algorithm that is accurate to very low frequencies," *Appl. Computat. Electromagn. Soc. J.*, vol. 10, pp. 58–68, Nov. 1995.

[7] W. Wu, A. W. Glisson, and D. Kajfez, "A study of two numerical solution procedures for the electric field integral equation at low frequency," *Appl. Computat. Electromagn. Soc. J.*, vol. 10, pp. 69–80, Nov. 1995.

[8] G. Vecchi, "Loop-star decomposition of basis functions in the discretization of EFIE," *IEEE Trans. Antennas Propag.*, vol. 47, no. 2, pp. 339–346, Feb. 1999.

[9] J. F. Lee, R. Lee, and R. J. Burkholder, "Loop star basis functions and a robust preconditioner for EFIE scattering problems," *IEEE Trans. Antennas Propag.*, vol. 51, no. 8, pp. 1855–1863, Aug. 2003.

[10] T. F. Eibert, "Iterative-solver convergence for loop-star and loop-tree decomposition in method-of-moments solutions of the electric-field integral equation," *IEEE Antennas Propag. Mag.*, vol. 46, no. 6, pp. 80–85, Jun. 2004.

[11] R. J. Adams, "Physical and analytical properties of a stabilized electric field integral equation," *IEEE Trans. Antennas Propag.*, vol. 52, no. 2, pp. 362–372, Feb. 2004.

[12] H. Contopanagos, B. Dembart, M. Epton, J. J. Ottusch, V. Rokhlin, J. L. Fisher, and S. M. Wandzura, "Well-conditioned boundary integral equations for three-dimensional electromagnetic scattering," *IEEE Trans. Antennas Propag.*, vol. 50, no. 12, pp. 1824–1830, Dec. 2002.

[13] S. Borel, D. P. Levadoux, and F. Alouges, "A new well-conditioned integral formulation for maxwell equations in three dimensions," *IEEE Trans. Antennas Propag.*, vol. 53, no. 9, pp. 2995–3004, Sep. 2005.

[14] R. J. Adams and N. J. Champagne II, "A numerical implementation of a modified form of the electric field integral equation," *IEEE Trans. Antennas Propag.*, vol. 52, no. 9, pp. 2262–2266, Sep. 2004.

[15] F. P. Andriulli, K. Cools, H. Bagci, F. Olyslager, A. Buffa, S. Christiansen, and E. Michielssen, "A multiplicative Calderón preconditioner for the electric field integral equation," *IEEE Trans. Antennas Propag.*, vol. 56, no. 8, pp. 2398–2412, Aug. 2008.

[16] A. Buffa and S. Christiansen, "A dual finite element complex on the barycentric refinement," *Math. Comput.*, vol. 76, no. 260, pp. 1743–1769, Oct. 2007.

[17] H. Bagci, F. P. Andriulli, K. Cools, F. Olyslager, and E. Michielssen, "A Calderón multiplicative preconditioner for the combined field integral equation," *IEEE Trans. Antennas Propag.*, vol. 57, no. 10, pp. 3387–3392, Oct. 2009.

[18] F. Valdés, F. P. Andriulli, H. Bagci, and E. Michielssen, "A Calderón-preconditioned single source combined filed integral equation for analyzing scattering from homogeneous penetrable objects," *IEEE Trans. Antennas Propag.*, vol. 59, no. 6, pp. 2315–2328, Jun. 2011.

[19] Q. L. Chen and D. R. Wilton, "Electromagnetic scattering by three-dimensional arbitrary complex material/conducting bodies," in *IEEE Int. Symp. on Antennas and Propag.*, 1990, vol. 2, pp. 590–593.

[20] M. S. Tong, W. C. Chew, B. J. Rubin, J. D. Morsey, and L. Jiang, "On the dual basis for solving electromagnetic surface integral equations," *IEEE Trans. Antennas Propag.*, vol. 57, no. 10, pp. 3136–3146, Oct. 2009.

[21] Q. L. Chen, "Electromagnetic Modeling of Three-Dimensional Piecewise Homogeneous Material Bodies of Arbitrary Composition and Geometry," Ph.D. dissertation, Dept. Electr. Eng., Univ. Houston, Houston, TX, 1990.

[22] M. B. Stephanson and J.-F. Lee, "Preconditioner electric field integral equation using Calderón identities and dual loop/star basis functions," *IEEE Trans. Antennas Propag.*, vol. 57, no. 4, pp. 1274–1279, Apr. 2009.

[23] S. Yan, J.-M. Jin, and Z. Nie, "EFIE analysis of low-frequency problems with loop-star decomposition and Calderón multiplicative preconditioner," *IEEE Trans. Antennas Propag.*, vol. 58, no. 3, pp. 857–867, Mar. 2010.

[24] J. Peeters, I. Bogaert, K. Cools, J. Fostier, and D. D. Zutter, "Combining Calderón preconditioning with fast multipole methods," in *IEEE Int. Symp. on Antennas and Propag.*, Toronto, Ontario, Canada, Jul. 2010.
[25] Y. Zhang, T. J. Cui, W. C. Chew, and J.-S. Zhao, "Magnetic field integral equation at very low frequencies," *IEEE Trans. Antennas Propag.*, vol. 51, no. 8, pp. 1864–1871, Aug. 2003.
[26] C. M. Bender and S. A. Orszag, *Advanced Mathematical Methods for Scientists and Engineers: Asymptotic Methods and Perturbation Theory*. New York: Springer, 1999.
[27] Z.-G. Qian and W. C. Chew, "Enhanced A-EFIE with perturbation method," *IEEE Trans. Antennas Propag.*, vol. 58, no. 10, pp. 3256–3264, Oct. 2010.
[28] Z.-G. Qian and W. C. Chew, "An augmented electric field integral equation for low frequency electromagnetics analysis," presented at the IEEE Int. Symp. on Antennas and Propag., San Diego, CA, Jul. 2008.
[29] Z.-G. Qian and W. C. Chew, "An augmented EFIE for high speed interconnect analysis," *Micro. Opt. Technol. Lett.*, vol. 50, no. 10, pp. 2658–2662, Oct. 2008.
[30] Z.-G. Qian and W. C. Chew, "Fast full-wave surface integral equation solver for multiscale structure modeling," *IEEE Trans. Antennas Propag.*, vol. 57, no. 11, pp. 3594–3601, Nov. 2009.
[31] G. Vecchi, L. Matekovits, P. Pirinoli, and M. Orefice, "Application of numerical regularization options to integral-equation analysis of printed antennas," *IEEE Trans. Antennas Propag.*, vol. 45, no. 3, pp. 570–572, Mar. 1997.
[32] G. C. Hsiao and R. E. Kleinman, "Mathematical foundations for error estimation in numerical solutions of integral equations in electromagnetics," *IEEE Trans. Antennas Propag.*, vol. 45, no. 3, pp. 316–328, Mar. 1997.
[33] K. Cools, F. P. Andriulli, F. Olyslager, and E. Michielssen, "Nullspaces of MFIE and Calderón preconditioned EFIE operators applied to toroidal surfaces," *IEEE Trans. Antennas Propag.*, vol. 57, no. 10, pp. 3205–3215, Oct. 2009.
[34] I. Bogaert, K. Cools, F. P. Andriulli, and D. De Zutter, "Low frequency scaling of the mixed MFIE for scatterers with a non-simply connected surface," in *Proc. Int. Conf. on Electromagn. in Advanced Appl.*, Sep. 2011, pp. 951–954.

Sheng Sun (S'02–M'07–SM'12) received the B.Eng. degree in information and communication engineering from Xi'an Jiaotong University, Xi'an, China, in 2001, and the Ph.D. degree in electrical and electronic engineering from the Nanyang Technological University, Singapore, in 2006.

He was with the Institute of Microelectronics in Singapore (2005–2006), and with the School of Electrical and Electronic Engineering at the Nanyang Technological University in Singapore (2006–2008). Previously, he was a Humboldt Research Fellow with the Institute of Microwave Techniques at the University of Ulm in Germany (2008–2010). Since 2010, he has been a Research Assistant Professor with the Department of Electrical and Electronic Engineering at The University of Hong Kong. His research interests include electromagnetic theory and computational methods, numerical modeling and de-embedding techniques, electromagnetic wave propagation and scattering, microwave and millimeter-wave radar system, as well as the study of multilayer planar circuits, microwave filters and antennas. He has coauthored a book entitled *Microwave Bandpass Filters for Wideband Communications*, authored and coauthored over 60 journal and conference publications.

Dr. Sun received the Outstanding Reviewer Award for the IEEE MICROWAVE AND WIRELESS COMPONENTS LETTERS (2010). He was the recipient of a Hildegard Maier Research Fellowship of the Alexander Von Humboldt Foundation in Germany (2008). He was also the recipient of the Young Scientist Travel Grant presented at the International Symposium on Antennas and Propagation in Japan (2004), and the NTU Research Scholarship in Singapore (2002–2005). He is currently an associate editor for the *IEICE Transactions on Electronics*.

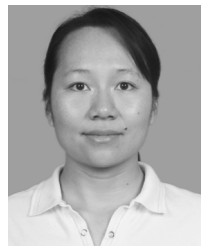

Yang G. Liu was born in Henan, China, in 1981. She received the B.S. degree in mathematics from the Zhengzhou University, Zhengzhou, China, in 2002, and the Ph.D. degree in computational mathematics from the Academy of Mathematics and Systems Science, Chinese Academy of Sciences, Beijing, China, in 2007.

From 2007 to 2011, she was a Postdoctoral Research Fellow with the Department of Electrical and Electronic Engineering, The University of Hong Kong. Since August 2011, she has been an Assistant Professor with the Institute of Applied Physics and Computational Mathematics, Beijing, China. Her research interests are computational electromagnetics, integral equation methods, fast multiple algorithms, finite element method, as well as domain decomposition methods.

Weng Cho Chew (S'79–M'80–SM'86–F'93) received the B.S. degree in 1976, both the M.S. and Engineer's degrees in 1978, and the Ph.D. degree in 1980, from the Massachusetts Institute of Technology, Cambridge, all in electrical engineering.

He has been with the University of Illinois since 1985. He served as the Dean of Engineering at The University of Hong Kong (2007–2011). Previously, he was the Director of the Center for Computational Electromagnetics and the Electromagnetics Laboratory at the University of Illinois (1995–2007). Before joining the University of Illinois, he was a Department Manager and a Program Leader at Schlumberger-Doll Research (1981–1985). His research interests are in the areas of wave physics and mathematics in inhomogeneous media for various sensing applications, integrated circuits, microstrip antenna applications, and fast algorithms for solving wave scattering and radiation problems. He is the originator several fast algorithms for solving electromagnetics scattering and inverse problems. He led a research group that developed computer algorithms and codes that solved dense matrix systems with tens of millions of unknowns for the first time for integral equations of scattering. He has authored a book entitled *Waves and Fields in Inhomogeneous Media*, coauthored two books entitled *Fast and Efficient Methods in Computational Electromagnetics*, and *Integral Equation Methods for Electromagnetic and Elastic Waves*, authored and coauthored over 300 journal publications, over 400 conference publications and over ten book chapters.

Dr. Chew is a Fellow of IEEE, OSA, IOP, Electromagnetics Academy, Hong Kong Institute of Engineers (HKIE), and was an NSF Presidential Young Investigator (USA). He received the Schelkunoff Best Paper Award for AP Transaction, the IEEE Graduate Teaching Award, UIUC Campus Wide Teaching Award, IBM Faculty Awards. He was a Founder Professor of the College of Engineering (2000–2005), and the First Y.T. Lo Endowed Chair Professor (2005–2009). He has served as an IEEE Distinguished Lecturer (2005–2007), the Cheng Tsang Man Visiting Professor at Nanyang Technological University in Singapore (2006). In 2002, ISI Citation elected him to the category of Most-Highly Cited Authors (top 0.01%). He was elected by IEEE AP Society to receive the Chen-To Tai Distinguished Educator Award (2008). He is currently the Editor-in-Chief of JEMWA/PIER journals, and on the Board of Directors of Applied Science Technology Research Institute, Hong Kong. He served on the IEEE Adcom for Antennas and Propagation Society as well as Geoscience and Remote Sensing Society. He has been active with various journals and societies.

Zuhui Ma received the B.S. and M.S. degrees in microwave engineering from the University of Electronic Science and Technology of China (UESTC), Chengdu, in 2006 and 2009, respectively. He is currently working towards the Ph. D. degree in electrical and electronic engineering in the University of Hong Kong, Hong Kong, China.

His research interests include numerical methods and fast algorithms in computational electromagnetics.